



Long-term Brown Carbon and Smoke Tracer Observations in Bogotá, Colombia: Association to Medium-Range Transport of Biomass Burning Plumes

Juan Manuel Rincón-Riveros¹, Maria Alejandra Rincón-Caro¹, Amy P. Sullivan², Juan Felipe Mendez-Espinosa¹, Luis Carlos Belalcazar³, Miguel Quirama Aguilar¹, and Ricardo Morales Betancourt¹

¹Civil and Environmental Engineering Department, Universidad de los Andes, Bogotá, Colombia

²Department of Atmospheric Science, Colorado State University, Fort Collins, CO, USA

³Universidad Nacional de Colombia, Bogotá, Colombia

Correspondence: Ricardo Morales Betancourt (r.moralesb@uniandes.edu.co)

Abstract. Light-absorbing aerosols emitted during open biomass burning (BB) events such as wildfires and agricultural burns have a strong impact on the Earth's radiation budget through both direct and indirect effects. Additionally, BB aerosols and gas-phase emissions can substantially reduce air quality at local, regional, and global scales, negatively affecting human health. South America is one of largest contributors to BB emissions globally. After Amazonia, the BB emissions from the wildfires and agricultural burns in the grassland plains of Northern South America (NSA) are the most significant in the region. However, few studies have analyzed the potential impact of NSA BB emissions on regional air quality. Recent evidence suggests that seasonal variations in air quality in several major cities in NSA could be associated with open biomass burning emissions, but it is still uncertain to what those sources impact air quality in the region. In this work, we report on 3 years of continuous equivalent Black Carbon (eBC) and Brown Carbon (BrC) observations at a hill-top site located upwind of the city of Bogotá and we demonstrate its association with MODIS detected fires in a 3000 km x 2000 km domain. Off-line PM_{2.5} filter samples collected during three field campaigns were analyzed to quantify water-soluble organic carbon (WSOC), organic and elemental carbon (OC/EC), and biomass burning tracers such as levoglucosan, galactosan, and potassium. MODIS Active Fire Data and HYSPLIT back-trajectories were used to identify potential biomass burning plumes transported to the city. We analyzed the relationship between BrC, WSOC, water-soluble potassium, and levoglucosan to identify signals of regional transport of BB aerosols. Our results confirm that regional biomass burning transport from wildfires occurs annually during the months of January and April. The seasonality of eBC followed closely that of PM_{2.5} at the city air quality stations, however, the observed seasonality of BrC is distinctly different to that of eBC and strongly associated to regional fire counts. The strong correlation between BrC and regional fire counts was observed both at daily, weekly, and monthly time-scales. WSOC at the measurement site was observed to increase linearly with levoglucosan during high BB periods, and to remain constant at $\sim 2.5 \mu\text{gC m}^{-3}$ during the low BB activity seasons. Our findings show, for the first time in this region, that aged BB plumes can regularly reach densely populated areas in the Central Andes of Northern South America. A source footprint analysis involving BrC



observations, back-trajectories, and remotely sensed fire activity shows that the eastern savannas in NSA are the main BB source region for the domain analyzed.

25 1 Introduction

Open biomass burning is a significant source of atmospheric aerosol particles and gas-phase pollutants (e.g., Bond et al., 2004; Aurell and Gullett, 2013; Tsimpidi et al., 2016). The particles emitted during biomass burning (BB) have a complex chemical composition dominated by primary organic matter (POM), elemental carbon (EC), and inorganic material such as sulfates, nitrates, and potassium (e.g., Yamasoe et al., 2000; Akagi et al., 2011). These species can contribute to deteriorated air quality levels in urban centers (e.g., Phuleria et al., 2005; Garcia-Hurtado et al., 2014; Kollanus et al., 2016). The impacts of BB plumes over air quality for sites located several thousand kilometers away from the BB sources has been demonstrated (e.g., Forster et al., 2001; Cottle et al., 2014). Many studies have documented the negative effects of BB emissions over human health (Youssef et al., 2014; Haikerwal et al., 2015; Reid et al., 2016). Additionally, the typically internally mixed carbonaceous components of BB particles contribute significantly to absorption of visible and UV light (Kirchstetter et al., 2004). Due to its strong absorption of visible light, EC is sometimes measured through light-absorption techniques, and is referred to as equivalent Black Carbon (eBC) (Petzold et al., 2013). However, the organic material (OM) present in BB particles has a strong absorption in UV wavelengths, and this absorption increases proportionally to the amount of OM present in the aerosol. The collection of light-absorbing organic compounds present in BB particles are termed Brown Carbon (BrC) (e.g., Kirchstetter et al., 2004; Wang et al., 2018). Therefore, the aerosol particles emitted to the atmosphere through BB are the most significant short-lived climate pollutant and are the second largest contributors to anthropogenic radiative forcing (Stohl et al., 2015; Bond et al., 2013).

Biomass burning emissions from South America contribute the most to the global BC inventory, with 16% of the global emissions, surpassing those of other critical areas such as Asia and Africa (e.g., Koch et al., 2007; van der Werf et al., 2010). In particular, the Brazilian Amazonia and Cerrado regions produce substantial BB emissions, whose impacts have been the subject of numerous studies (e.g., Crutzen and Andreae, 1991; de Oliveira Alves et al., 2015; Gonçalves et al., 2016). Emissions from Amazonia and Cerrado occur typically between May and September, which corresponds to the dry season in the region (Marengo et al., 2011). Fires in the savannas and tropical forests thousands of kilometers north of the Brazilian Amazonia, an area known as Northern South America (NSA), can also have significant global and local impacts (van der Werf et al., 2010). However, due to the significance of the BB emission from Amazonia, emissions from NSA have often been overlooked despite its potential impacts on air quality and climate (Thornhill et al., 2017). The equatorward location of NSA causes its annual precipitation and BB emissions patterns to differ strongly from those of Amazonia. Peak emissions in the former occur between January and April with minimum BB activity between June and October. Those BB activity patterns in NSA are



mostly determined by the dynamics of wet and dry seasons, which are in turn controlled by the annual south-north migration of the Intertropical Convergence Zone (ITCZ) (Pulwarty et al., 1998; Poveda et al., 2006; Mendez-Espinosa et al., 2019). Inter-annual variability in the intensity and length of the dry season, controlled by El Niño Southern Oscillation (ENSO), modulates the intensity of the peak BB emissions in NSA (Poveda et al., 2006).

The BB plumes generated in these fires can negatively impact the air quality experienced by over 60 million people that live, mostly in the urban areas, in Venezuela, Colombia, and Ecuador. Only recently some studies have focused on the air quality impacts of BB emissions in this region. Observational studies performed at *Pico Espejo* mountain (Venezuela), over 4000 m in altitude, detected the passage of BB plumes during the dry season (Hamburger et al., 2013). Because of its vertical elevation, the *Pico Espejo* site often sampled free-troposphere aerosols, showing the potential long-range transport of aged BB plumes (Schmeissner et al., 2011). More recently, $PM_{2.5}$ and ozone observations in the sparsely populated savannas in NSA showed extremely high concentrations even in small towns where measurements were performed (Hernandez et al., 2019). These high $PM_{2.5}$ and ozone levels were associated with distant fires in the Venezuelan savannas. The potential regional-scale air quality impacts of BB emissions in NSA was recently explored by (Mendez-Espinosa et al., 2019). In their work a systematic analysis of air mass back-trajectories and MODIS hotspots for a ten-year period was conducted, finding a strong association between fire counts in NSA and $PM_{2.5}$ concentrations in cities located hundreds of kilometers from the BB sources. Mendez-Espinosa et al. (2019) showed that BB emissions from the NSA savannas could be transported westward impacting air quality in several large metropolitan areas. However, there were no direct measurements of BB available to confirm the presence of BB aerosols in the urban areas considered. Since the main BB source regions are located hundreds of kilometers from the most densely populated areas, the BB plumes are likely aged. Atmospheric aging of BB aerosols has been shown to increase the oxidative potential of the particles (e.g., Wong et al., 2019), potentially increasing the particles toxicity in addition to contributing to aerosol mass.

Detection of BB aerosols using chemical tracers is necessary to confirm the contribution of fires to aerosol loading at a given location. Traditionally potassium (K), levoglucosan, BrC, water-soluble organic carbon (WSOC), and other species have been used as biomass burning particle tracers (e.g., Sullivan and Weber, 2006a, b; Laskin et al., 2015; Shen et al., 2017; Martinsson et al., 2017). Potassium, *K*, has been extensively used as a BB tracer but there are significant non-biomass burning related sources of K, and it does not always correlate well with BB smoke (Pachón et al., 2013). Levoglucosan and other anhydrosugars, which are formed through the pyrolysis of cellulose, are more specific BB tracers (Simoneit et al., 1999). A potential limiting factor in the use of levoglucosan as a BB tracer is its oxidation in the atmosphere, with a lifetime of a few days when exposed to OH radical (Hennigan et al., 2010), reducing its abundance in long-range transported BB plumes that have aged substantially in the atmosphere. Furthermore, Aerosol Mass Spectrometer data has shown that mass fractions associated with Levoglucosan correlate strongly with light-absorbing carbonaceous material (e.g., Cubison et al., 2011; Lack et al., 2013). BB is also a significant primary source of WSOC (Sullivan and Weber, 2006b), but WSOC can also be formed through gas-to-particle conversion of gas-phase organics (e.g., Weber et al., 2007). WSOC has also been shown to be a strong absorber in the UV part of the spectrum, as indicated by measurements of absorption Angstrom exponent from filter extracts



(Hecobian et al., 2010). Because of the optically active components, BB aerosols can be detected through multi-wavelength particle light absorption measurements (e.g., Jeong et al., 2004).

In this work, we determine for the first time, to our knowledge, the presence of BB plumes in a large metropolitan area in NSA by using long-term observations of BB tracers. We linked the smoke tracer observations with regional BB activity, showing the role of medium-range transport of BB plumes in urban air pollution in Northern South America. We approach this problem by carrying out measurements on a hill-top site near Bogotá, Colombia. Continuous Brown Carbon and Black Carbon observations during a three-year period were used to establish temporal patterns in the BB tracer signal. The potential origin of the BB aerosols at the site was explored by analyzing the time series of MODIS active fire data in the NSA domain together with a systematic back-trajectory analysis (Mendez-Espinosa et al., 2019). Specific smoke tracers such as levoglucosan and water-soluble potassium were quantified. Our results show that smoke tracers in Bogotá are strongly associated with regional BB activity. The wildfires and agricultural burns in NSA from January to April contributes particularly to OC and WSOC concentration in the city of Bogotá.

2 Methods

We measured BrC and eBC continuously during a three year period at a hill-top site located in Bogotá, Colombia. Filter-based aerosol samples were also collected at the site over three different field campaigns spanning both, high and low BB activity in NSA. These samples were analyzed for smoke markers such as levoglucosan and other sugars. Water-soluble organic carbon (WSOC), inorganic ions, and EC/OC were also measured from the filter samples. Additionally, we combined MODIS active fire data with back-trajectory analysis to explore the potential transport of BB affected air masses

2.1 Measurement site description

The broader study domain covers a vast area of nearly 3.9 million km² (Figure 1a). The western part of NSA, dominated by the Andes mountain range, is a densely populated region with more than 60 million inhabitants. The eastern part of NSA includes the tropical grasslands and woodlands plains of the Orinoco river basin. The Orinoco river basin is sparsely populated and its economic activity is based on agricultural activities. The annual cycle of precipitation over the region is controlled by the meridional displacement of the ITCZ (Poveda et al., 2006). The ITZC southernmost location occurs typically during DJF. These months, are therefore characterized by dryer weather in NSA as the deep convection areas are displaced southward, towards Amazonia (Mendez-Espinosa et al., 2019). This mechanisms in turn, largely explain the BB activity patterns in the region.

The measurement instruments were deployed at the *Monserate* Sanctuary (Long. = -74.05649°, Lat. = 4.60582°). This Sanctuary is located on a hill-top on the Eastern margin of the urban perimeter of Bogotá, Colombia (Figure 1b). The altitude of the *Monserate* site is 3152 m above sea level, and 550 m above the mean height of the Andean plateau were the city of Bogotá lies (Figure 1). Easterly winds prevail at the site, placing it upwind from the densely populated metropolitan area with 9 million people (Figure 1b). According to the Air Quality monitoring stations in the city, annual average PM_{2.5} concentration



was $19 \mu\text{g m}^{-3}$ during 2018, with a strong seasonal cycle in which monthly-mean $\text{PM}_{2.5}$ between February and March can reach $35 \mu\text{g m}^{-3}$ and decrease to $11 \mu\text{g m}^{-3}$ in July. Primary aerosol emissions are estimated to be 2600 tons/year, with a substantial contribution from diesel powered public transport buses and cargo trucks (Pachón et al., 2018). Road dust re-suspension emissions are highly uncertain, but are thought to contribute significantly to primary emissions (Pachón et al., 2018). There are no significant emission sources or urbanized areas West of the city (Figure 1b). Therefore, the measurement site location was intended to minimize the impact from the urban back-ground and allowing the detection of regional signals.

125 Wind speed and direction, UV radiation, relative humidity, and barometric pressure were also recorded on-site with a frequency of 10 minutes (Davis Advantage Pro II).

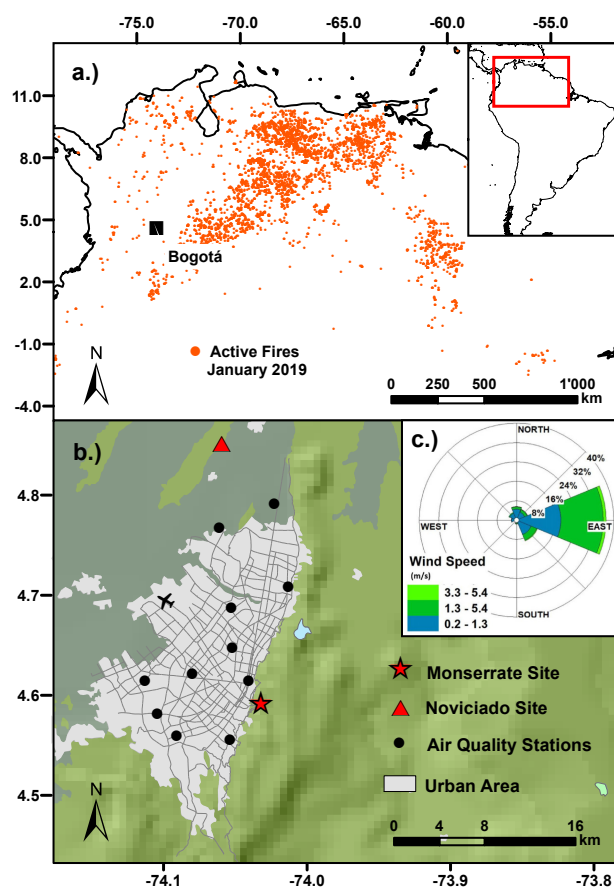


Figure 1. (a.) Geographic location of the Northern South America (NSA) domain as defined in this study and locations of MODIS hotspots during January 2019. The inset shows the location of NSA relative to South America (b.) Location of the *Monserrate* Sanctuary site (star) near Bogotá and the AQ stations (filled circles). (c.) Wind direction observed at *Monserrate* hill-top site during the period May/2016 - Apr/2019



2.2 BrC and BC measurements

Aerosol light absorption coefficient, b_{abs} (Mm^{-1}), was measured continuously using a 7-wavelength (370, 470, 520, 590, 660, 880, 950 nm), Aethalometer (Aerosol inc., model AE-33) described by Drinovec et al. (2015). The measurements were carried out at the *Montserrat* Sanctuary site during the three-year period from May 2016 - April 2019. Data was logged every 60 seconds. The sampling rate was 2 LPM through a $PM_{1.0}$ inlet (BGI model SCC0.732) to avoid potential mineral dust absorption interference on the measurements since most of either fresh or aged BB aerosol particles are in the sub-micrometer size range (Janhäll et al., 2010). The b_{abs} raw data was corrected to account for filter loading effects (Virkkula et al., 2007). The correction parameter for each wavelength, k_λ , is automatically computed by the instrument by asymmetrically splitting the sample flow and simultaneously measuring attenuation at two differentially loaded filter spots (Drinovec et al., 2015). Equivalent black carbon concentration, eBC ($\mu g m^{-3}$), was computed from corrected b_{abs} measured at the 880 nm channel using a mass absorption cross-section $\sigma = 7.77 m^2 g^{-1}$ and a multiple scattering parameter $C = 1.57$, i.e., $eBC = b_{abs} / (C \times \sigma)$. The estimated eBC limit of detection was $40 ng m^{-3}$ for a 1 hour interval. A lower limit of detection is achieved with longer integration periods.

The spectral dependence of b_{abs} was characterized with the Angstrom Absorption Exponent, α , which is the logarithmic slope of the relation between b_{abs} and wavelength, λ , i.e.,

$$\frac{b_{abs}(\lambda_1)}{b_{abs}(\lambda_2)} = \left(\frac{\lambda_1}{\lambda_2}\right)^{-\alpha} \quad (1)$$

where $b_{abs}(\lambda_i)$ is the absorption coefficient at wavelength λ_i . Several different methods to apportion absorption to either fossil fuels or biomass burning have been developed (e.g., Sandradewi et al., 2008; Massabò et al., 2015; Chen et al., 2018). In this work, deconvolution of b_{abs} between the contribution from fossil fuel and from biomass burning was done by applying the two-component model described by Sandradewi et al. (2008). In their model, aerosol absorption at any given wavelength can be separated into the contribution of BB aerosol absorption and fossil fuels, i.e., $b_{abs}(\lambda) = b_{abs, BB}(\lambda) + b_{abs, FF}(\lambda)$. Furthermore, it is assumed that the spectral dependence of absorption for each component is characterized by a specific Angstrom exponent. This is, $b_{abs, BB} \sim \lambda^{\alpha_{BB}}$ and $b_{abs, FF} \sim \lambda^{\alpha_{FF}}$. Many studies suggest that $\alpha_{FF} = 1$ (e.g., Lack and Langridge, 2013), however, there is large variability in published Angstrom exponent values associated to BrC (e.g., Hecobian et al., 2010; Harrison et al., 2013; Lack and Langridge, 2013). In this work we used $\alpha_{FF} = 1$ and $\alpha_{BB} = 2$ as has been suggested in several studies. Equation 1 was then applied to b_{abs} measured at 470 nm and 880 nm wavelengths to compute an observed α . The fraction of light-absorbing aerosol attributable to BB, i.e., f_{BB} , is inferred from α by applying the two-component model (Sandradewi et al., 2008), i.e.,

$$f_{BB} = 1 - \left(\frac{\lambda_1}{\lambda_2}\right)^{1-\alpha_{FF}} \frac{\left(\frac{\lambda_1}{\lambda_2}\right)^{\alpha_{BB}-\alpha} - 1}{\left(\frac{\lambda_1}{\lambda_2}\right)^{\alpha_{BB}-\alpha_{FF}} - 1} \quad (2)$$



We assumed f_{BB} to be zero for $\alpha \leq \alpha_{FF}$ and one for $\alpha \geq \alpha_{BB}$. Brown Carbon concentration is then computed as $\text{BrC} = e\text{BC} \times f_{BB}$.

2.3 Biomass Burning Tracers

160 Filter-based aerosol samples were collected during three different field campaigns (Table 1) at the *Monserate* site described in Section 2.1. The campaigns were designed to span high and low BB activity periods in NSA. Two of these campaigns were carried out during the high BB activity season (Campaigns 1 and 3) from January to April of 2018 and 2019, respectively, and one campaign was carried out during NSA rainy season (Campaign 2) from July to September 2018. Samples were collected onto 37 mm quartz filters for 24 hour periods (starting at midnight) every other day using a low-volume sampler. The sampler
165 has a $\text{PM}_{2.5}$ inertial impaction stage and a sampling flow rate of 10 LPM. A total of 88 samples were collected and analyzed to quantify BB tracers on the aerosol samples. Blank samples at each sampling site were also analyzed. These handling blank filters were carried to the sampling site and placed in the sampling instrument with the vacuum pump turned off.

Table 1. $\text{PM}_{2.5}$ sampling campaigns carried out on *Monserate* Site, where N stands for the number of filter samples

Campaign ID	Sampling Period	N
1. High-BB	2018/01/15 - 2019/04/15	31
2. Low-BB	2018/07/15 - 2019/09/15	24
3. High-BB	2019/01/15 - 2019/04/15	33

The quartz filters were pre-baked at 550°C for 12 hours to reduce their organic background and later placed in a desiccator to prevent water vapor absorption. After sampling, the filters were stored in a freezer at -80°C in plastic Petri dishes. At the end
170 of each field campaign samples were sent over-night in a refrigerated container for chemical analysis to the Collett Laboratory at Colorado State University.

Organic carbon (OC) and elemental carbon (EC) were determined from a 1.4 cm^2 punch in each filter using a thermal/optical transmission (TOT) EC/OC semi-continuous analyzer (Sunset Labs Inc.) following the NIOSH Method 5040 (Birch and Cary, 1996). The LOD was $0.2\ \mu\text{gC m}^{-3}$ and $0.5\ \mu\text{gC m}^{-3}$ for OC and EC, respectively. The remainder of the 37 mm filter was
175 extracted in 15 ml of deionized water, and the extracts filtered with $0.2\ \mu\text{m}$ PTFE syringe filter to remove insoluble particles. Water-soluble organic carbon (WSOC) was measured with a TOC analyzer (Siervers Model M9 Turbo). This instrument measures WSOC by converting all organic carbonaceous material in the water extract to carbon dioxide using chemical oxidation by ultraviolet light (UV) and ammonium persulfate. The LOD for WSOC in this study was $0.1\ \mu\text{gC m}^{-3}$. The overall measurement uncertainties for compounds analyzed is estimated to be $\sim 10\%$ (Sullivan et al., 2008).

180 A fraction of the aqueous extract was used to analyze for carbohydrates (including levoglucosan) through High-Performance Anion-Exchange Chromatography with Pulsed Amperometric Detection (HPAEC-PAD) (Sullivan et al., 2011). This technique uses a Dionex DX-500 series ion chromatograph with a Dionex GP-50 pump and a Dionex ED-50 electrochemical detector



operating in integrating amperometric mode using waveform A. Detailed descriptions of this method can be found elsewhere (e.g., Sullivan et al., 2008, 2011). The LOD for carbohydrates quantification is less than $\sim 0.1 \text{ ng/m}^3$.

185 Another portion of the aqueous extract was used to quantify inorganic anions and cations, including water-soluble potassium (WSK). For this analysis we used a Dionex ICS-3000 ion chromatograph with a conductivity detector, a isocratic pump and self-regenerating cation/anion suppressor. Cations were separated using a Dionex IonPac CS12A analytical column with a flowrate at 0.5 mL min^{-1} of 20 mM methanesulfonic acid eluent. The LOD for the various cations was $0.02 \text{ } \mu\text{g m}^{-3}$. In the case of anions, a Dionex IonPac AS11-HC anion-exchange column with a flowrate at 1.5 mL min^{-1} of sodium hydroxide
190 eluent was employed. The LOD for anions was $0.01 \text{ } \mu\text{g m}^{-3}$. This type of method has been applied by other studies (Tzompa-Sosa et al., 2016; Prenni et al., 2012) and further method details are presented by Sullivan et al. (2008).

2.4 Active Fires and Back-trajectory Analysis

MODerate-resolution Imaging Spectroradiometer (MODIS) observations were used to locate and count fires and its Fire Radiative Power (FRP) daily in the NSA domain (long. $=-79.0^\circ$, lat. $=-4.4^\circ$ as bottom left; long. $=-51.7^\circ$, lat. $=13.1^\circ$ as top right) during
195 May 2016 to April 2019. Only those active fires labeled with a $\geq 75\%$ confidence level were included in the analysis (Justice et al., 2002). The spatial distribution of fires during January 2019 is shown in Figure 1a, where the substantial dry-season BB activity on the eastern savannas of the Orinoco river basin can be seen.

We constructed several time series of daily fire counts, N_f , in the NSA domain by applying a variety of criteria. In the simplest criterion, all active fire counts in the domain, $N_{f,All}$, with confidence $\geq 75\%$ were considered. Next, a set of distance
200 criteria were applied and only the subset $N_{f,<R}$ of fire counts within a circular region with radius R from Bogotá were included. Time series considering radii of 200 km, 400 km, 600 km, 1000 km, and 1500 km were built following this method. Similarly, additional time series of only those fires in an annular region, N_{f,R_1-R_2} , defined by distances R_1 and R_2 were considered, i.e., those fires within $R_1 < R < R_2$.

MODIS active fire data was combined with Lagrangian back-trajectory analysis to explore the potential transport of BB
205 affected air masses following the methods of Mendez-Espinosa et al. (2019). Air-mass back trajectories arriving with three hour intervals (00:00, 03:00, 06:00, 09:00, 12:00, 15:00, 18:00 and 21:00 GMT-5) at Bogotá at 1000 m a.g.l., i.e., eighth daily, were computed using the NOAA HYSPLIT model (Stein et al., 2015; Draxler and Hess, 1998; Donnelly et al., 2015). Each trajectory was calculated for 96 hours prior to arrival in order to account for distant emission sources and avoid uncertainties on regional analysis due to longer trajectories (Donnelly et al., 2015). The Lagrangian trajectories were driven by GDAS1
210 meteorological fields (Su et al., 2015). The trajectory data was systematically analyzed using the OpenAir package (Carslaw and Ropkins, 2012) and the SplitR package of the open source programming language R. With this method, we constructed a time series of up-wind fire counts, $N_{f,upW}$, using an algorithm to select only upwind fires according to the trajectory analysis (Mendez-Espinosa et al., 2019). For this, a buffer zone of 150 km was defined around each of the 96 hourly locations defining one of the eight back-trajectories reaching the receptor city in any given day. Then, only active fires in these buffer zones were
215 included in the analysis. This method should account for any time lag between the occurrence of a fire and the effect over concentrations at a distant site. Additionally, time series of daily FRP data were constructed following the same procedures



described here for N_f . A statistical association analysis was then carried out between the data collected on-site, and the time series of fire counts and FRP. A source-footprint analysis was performed by combining the BrC observations, back-trajectories, and MODIS retrieved FRP (Supplementary Material).

220 2.5 $PM_{2.5}$ and eBC from the city monitoring stations

We retrieved $PM_{2.5}$ and eBC concentrations from the public air quality monitoring data repository of the Air Quality Monitoring Network of Bogotá. The air quality network data was then used to contrast the magnitude and temporal patterns of the measurements at the Monserrate Sanctuary site to those at the city. The $PM_{2.5}$ record from the air quality network covers the entire monitoring period but the eBC data covers only the last 9 months, since Aethalometers started operating on September 225 of 2018. The air quality network has eleven stations across the city with 6 of those currently monitoring eBC (Figure 1).

3 Results and Discussion

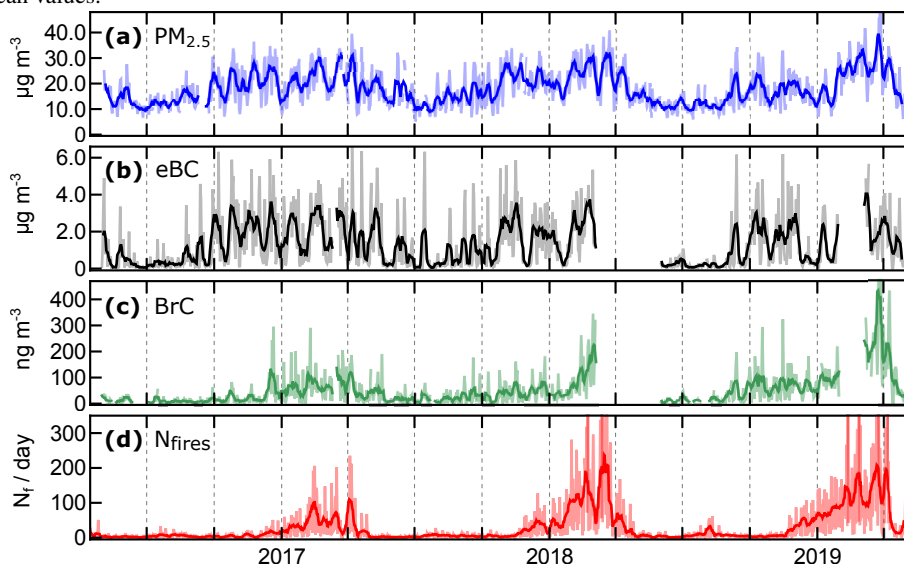
Equation 2 was applied as described in Section 2.2 to obtain eBC, f_{BB} , and BrC, with hourly and daily temporal resolution. The complete time-series of daily-mean observations of eBC and BrC at the hill-top site can be seen in Figure 2. Two short maintenance and calibration periods are seen in the data set as missing values. Observed daily-mean eBC concentration (Figure 230 2b) ranged from 0.02 to $5.0 \mu\text{g m}^{-3}$. BrC concentration were lower, with a maximum daily-mean of $0.44 \mu\text{g m}^{-3}$. During the 2018-2019 dry season (DJF) the highest f_{BB} was detected at the site, reaching up to 13% for the monthly mean for December and January. Additionally, daily-mean $PM_{2.5}$ retrieved from the AQ monitoring stations is shown in Figure 2a, and $N_{f,600-1000}$ constructed according to Section 2.4 is shown in Figure 2d.

Day to day variations in $PM_{2.5}$ and eBC at the Monserrate Site have a similar temporal pattern. A simple linear correlation analysis using the Spearman correlation between the two data sets, $\rho_{PM_{2.5}, eBC}$, confirms this relationship as $\rho_{PM_{2.5}, eBC} = 0.76$. 235 The similarity between both datasets shows that eBC measurements at the site are overwhelmingly dominated by EC emissions from urban traffic and industrial emissions. To examine the degree of influence of the city emissions at the measurement site we analyzed mixed layer height from daily radiosondes data at the airport station (SKBO station). We found that the Monserrate site is typically above the mixed layer early in the morning, up until 9:30 am when the mixing layer expands surpassing the 240 site altitude (Supplementary Material). Diurnal concentration patterns for eBC at the Monserrate Site and at the air quality monitoring stations support this hypothesis, since morning peak concentrations are observed with a lag of 1.5 to 2 hours at Monserrate compared to the city AQ stations (Supplementary Material).

In contrast, BrC data in Figure 2 has a significantly different temporal structure compared to both $PM_{2.5}$ and eBC. A correlation analysis shows a substantially lower correlation, $\rho_{PM_{2.5}, BrC} = 0.54$, compared to that of eBC and $PM_{2.5}$. This 245 difference in temporal patterns is indicative of a difference in the activity of sources of BrC and those of eBC, possibly suggesting that the BrC signal is controlled by BB outside of the city.



Figure 2. Time series of (a.) $\text{PM}_{2.5}$ ($\mu\text{g m}^{-3}$) from the Air Quality Monitoring Stations, (b.) equivalent Black Carbon ($\mu\text{g m}^{-3}$) from Monserrate Site, (c.) Brown Carbon ($\mu\text{g m}^{-3}$) from *Monserrate* Site, and (d.) Daily MODIS active fire counts in NSA within 600 km and 1000 km from Bogotá. Thick lines are seven-day moving averages from the original time series of daily-mean values. Faded lines in all panels show daily-mean values.



3.1 Monthly-mean BrC and eBC

The annual cycle observed for eBC at the Monserrate hill-top site (Figure 3a) is similar to that of $\text{PM}_{2.5}$ from the air quality stations (Figure 3b), with a bi-modal concentration pattern exhibiting maxima from February to March and from October to November. This seasonal pattern in $\text{PM}_{2.5}$ is in part explained by higher mixing heights during JJA and by lower mixing heights and increased static stability from December to March (Mendez-Espinosa et al., 2019). Monthly mean eBC at the Monserrate Site ranges from $0.25 \mu\text{g m}^{-3}$ in July to $1.70 \mu\text{g m}^{-3}$ during February and November. Consistent with what is observed at a daily time-scale, the similarity between the annual eBC and $\text{PM}_{2.5}$ variations is expected as the site is within the urban mixed layer during most of the day and therefore, heavily impacted by urban traffic emissions. Contrastingly, BrC seasonality is distinctly different from that of either eBC or $\text{PM}_{2.5}$, with a lone maximum from February to April and not exhibiting a second peak in the last months of the year (Figure 3b). This discrepancy between the seasonal cycles of BC and BrC further suggest that sources of both types of light-absorbing particles have different activity patterns along the year. Since eBC seems to be related to local emissions, the sources of BrC must be of a different type.

A potential explanation for the distinct seasonality of BrC at the site is found when analyzing the BB activity through MODIS active fire data after applying the fire counting algorithms described in Section 2.4. Figure 3b shows that the seasonality of BB activity is similar to that observed for BrC at the site, further suggesting a potential association between BB tracers in the city and regional BB activity.

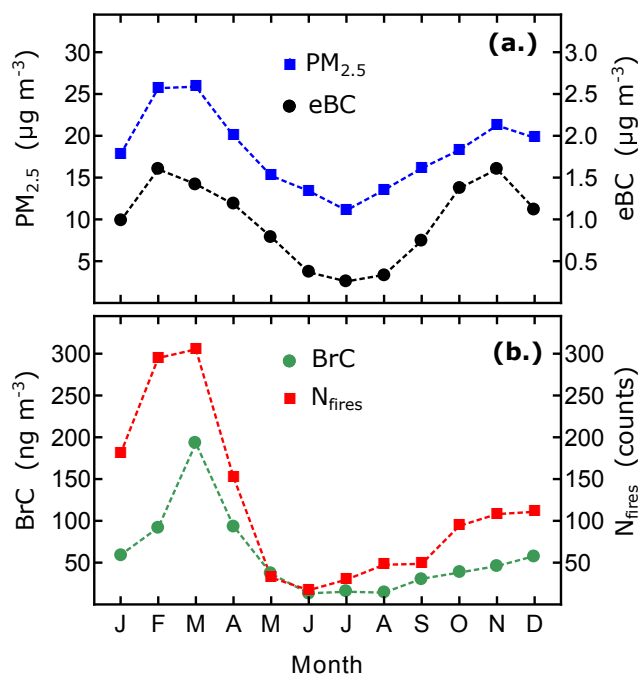


Figure 3. Monthly mean time series of Bogotá's $\text{PM}_{2.5}$ ($\mu\text{g m}^{-3}$), equivalent Black Carbon ($\mu\text{g m}^{-3}$), Brown Carbon ($\mu\text{g m}^{-3}$) and fire counts. The number of fire counts is the monthly mean of daily fire counts.

The distance of the most intense BB source areas in the eastern savannas and south-eastern tropical forests to the measurement site implies that the detected BB signal is due to aged biomass burning aerosols. This is supported by the high correlation with regional fire counts but the relatively low BrC concentration observed on site. The systematic increase in BrC during the first months of the year suggests that this is due to an increase in the contribution of BB aerosols to the regional background, rather than to sporadic episodes of high BB loading caused by transport of intense plumes.

3.2 Association with MODIS fire counts

To establish whether observed BrC at the *Montserrat* Site is related to regional BB activity, we performed a systematic statistical association analysis between BrC observations and the different fire counting methods described in Section 2.4. The Spearman correlation for the daily-mean as well as the seven-day moving average for eBC and BrC with N_f were calculated and summarized in Table 2. Overall, a weak statistical association was found between eBC and N_f , with values much lower than those observed between eBC and $\text{PM}_{2.5}$, confirming that a large fraction of eBC measured at the site is likely from local fossil fuel combustion sources. Furthermore, regardless of the fire counting scheme applied, the statistical association between BrC and N_f is stronger in all cases than that of eBC and N_f . Thus, despite the proximity of the measurement site to the city and the impact of local emissions, the association between regional BB activity in NSA and BrC suggest that the measurements at the site are able to differentiate the relatively small signal from regional BB to that of local emissions.



Table 2. Statistical association expressed through Spearman correlation between the different fire counting methods and eBC and BrC measured at Monserrate Site. Mov. Avg. is the Spearman correlation between smoothed time series with a seven-day moving average, and Daily are the Spearman correlations between daily-mean variables

MODIS fire counts	Brown Carbon		Black Carbon	
	Mov. Avg.	Daily	Mov. Avg.	Daily
$600 < R < 1000$ km	0.570	0.443	0.133	0.168
$400 < R < 600$ km	0.556	0.368	0.195	0.170
$R < 1000$ km	0.554	0.448	0.148	0.186
All-fires (>75%)	0.545	0.419	0.263	0.214
$R < 600$ km	0.521	0.369	0.167	0.163
$200 < R < 400$	0.495	0.334	0.171	0.178
$1000 < R < 1500$	0.454	0.251	0.095	0.035
Up-Wind fires	0.454	0.352	-0.063	-0.031
$R < 400$ km	0.453	0.316	0.114	0.152
$R < 200$ km	0.173	0.107	-0.096	0.005

Table 2 is ordered according to the Spearman correlation between the seven-day moving average fire counts and BrC. The result of the analysis shows a stronger association between BrC and distant fires, and the weakest association for those fires within 200 km of Bogotá. This is likely due to the substantially lower number of nearby fires compared to the abundant hot-spots in the Orinoco savannas and tropical forests. Therefore, either at a daily or weekly time-scales, the concentration of UV absorbing carbonaceous material in Bogotá is more closely associated with regional BB activity that with local emissions. The potentially more accurate fire counting method that only includes up-wind fires does not perform much better than the other methods considered. This result supports the idea that there is an increase in the regional BB aerosol background, decreasing the relative importance of direct advection of BB plumes. A spatial footprint analysis of BB source areas shows that in the period from December to March, the Orinoco savannas are likely the source regions impacting BrC at the Monserrate measurement site (see Supplementary Material).

3.3 Brown Carbon and Smoke Tracers

The continuous BrC measurements are a strong indicator of the enhanced presence of UV absorbing aerosols. However, optical methods are not always quantitative methods to determine BB aerosol loading. To establish the relationship between BrC and BB aerosols, we compared the 24-hour average BrC concentration with the concentration of smoke markers levoglucosan, galactosan, WSK, and WSOC, as well as EC. The analysis was done for those specific dates where collocated filter-based samples and optical BrC observations were available, totalling 58 valid dates. A strong linear association was found between BrC and levoglucosan ($R^2 = 0.87$, slope = 0.32), with the linearity spanning the full range of measurements (Figure 4a). This indicates that the optical measurements of BrC are indeed a good BB tracer.

Similarly strong associations were established for WSOC and other tracers (Table 3). When the association analysis is repeated only for data collected during the low-BB activity season (i.e., Campaign 2) the degree of association between BrC

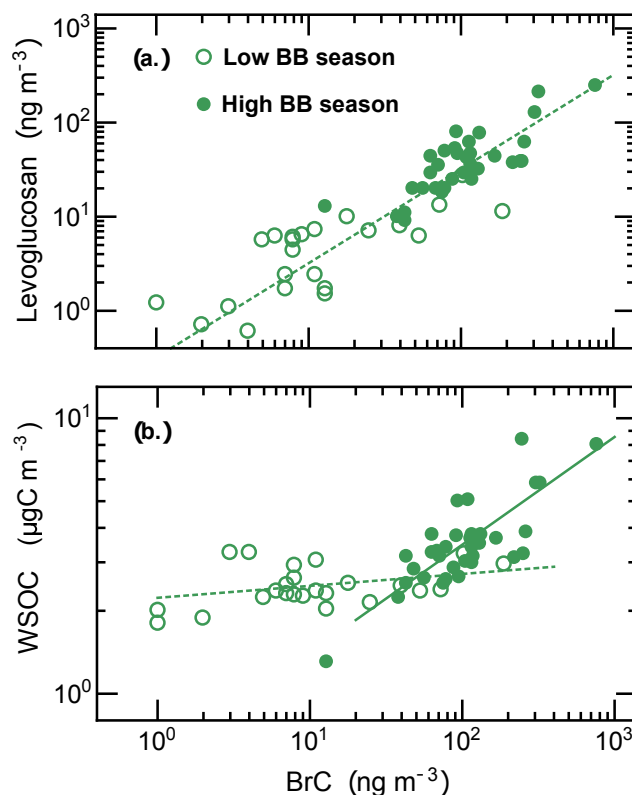


Figure 4. Scatter plot of daily-mean concentration of (a.) Levoglucosan and Brown Carbon, and (b.) WSOC and Brown Carbon, measured at the Monserrate site. Filled circles are samples collected during the high BB activity seasons, and open circles were collected during low BB activity.

Table 3. Spearman correlation between optical measurements of carbonaceous aerosols Brown Carbon (BrC) and Black Carbon (eBC) and selected smoke tracers levoglucosan (Lev.), galactosan (Gal.), WSOC, WSK, OC and EC measured at the Monserrate site. Correlation coefficients are shown for all data, as well as for the low and high BB seasons, respectively. *n* represents the number of samples.

		Lev.	Gal.	WSOC	WSK	OC	EC
All-data (n=58)	BrC	0.87	0.72	0.78	0.54	0.76	0.53
	eBC	0.35	0.36	0.53	0.41	0.60	0.97
High-BB (n=34)	BrC	0.85	0.70	0.75	0.46	0.69	0.38
	eBC	0.23	0.40	0.52	0.39	0.61	0.96
Low-BB (n=24)	BrC	0.66	0.60	0.34	0.13	0.52	0.88
	eBC	0.51	0.45	0.31	0.13	0.35	0.78

and WSOC drops significantly to just 0.34. This indicates that during low-BB activity months (JJA) WSOC has local sources likely not associated to BB. This is further supported by the much stronger association between levoglucosan and WSOC during high-BB seasons (0.73) compared to low-BB season (0.38). WSOC remained relatively constant between 2 and 3 $\mu\text{gC m}^{-3}$



during the low-BB activity season (Figure 4b), but increases more steeply as a function of BrC for the high-BB activity season. These observations suggest there are $2.5 \mu\text{gCm}^{-3}$ of WSOC not related to BB, and that during the high-BB season WSOC can reach up to $8 \mu\text{gCm}^{-3}$.

The observed levoglucosan concentrations are relatively low compared to what has been observed in other studies (Hecobian et al., 2010). However, the measured concentration of BB tracers are significant considering the distance between the measurement site and the source regions (see Supplementary Material).

4 Conclusions

In this study we determine for the first time the presence of medium-range transported biomass burning aerosols to urban areas in Northern South America by direct measurement of biomass burning tracers. The presence of BB burning affected air masses was confirmed by multi-wavelength optical measurements of Brown Carbon and Black Carbon, and by high-sensitivity detection of specific smoke tracers levoglucosan and galactosan. Continuous Brown Carbon measurements were performed during a three-year period with hourly time-resolution. These long-term observations allowed for the characterization of annual patterns in Black Carbon and Brown Carbon concentrations at the measurement site.

Despite the close proximity of the measurement site to the city center of a large, relatively polluted urban area, the statistical association between BrC and MODIS Active Fire data was strong on a daily basis. Furthermore, the association between BrC and fire counts was stronger for distant fires, i.e., those further than 400 km from the measurement site. This finding strongly supports the regional origin of the BB aerosol detected at the site. A source footprint analysis involving remotely sensed Fire Radiative Power data, back-trajectories calculations, and observed BrC concentration, further suggests that the eastern grasslands are the main biomass burning source region in NSA actually impacting populated urban areas. Our observations show that the annual pattern of Brown Carbon at the monitoring site was observed to have a single peak during February and March, coinciding with the peak in biomass burning activity in the region.

High-sensitivity levoglucosan, galactosan, and potassium measurements collocated with optical Brown Carbon observations were highly linearly correlated and showed excellent agreement. Therefore, the on-line optical observations at the measurement site were shown to be accurate tracers of BB aerosols when compared with well-established analytical methods. Water-soluble organic carbon (WSOC) was measured during high and low BB activity seasons. These observations suggest there are $2.5 \mu\text{gCm}^{-3}$ of WSOC not related to BB, and that BB can contribute to WSOC, at which time can reach up to $8 \mu\text{gCm}^{-3}$ for a 24 hour period.

The findings of this work demonstrate that background aerosol levels are increased every year due to the presence of aged biomass burning aerosols. The observed Brown Carbon and smoke tracer concentrations increase in close relation to the amount of MODIS detected fires. Despite the overwhelming black carbon signal coming from traffic emissions, a clear relation between the Brown Carbon signal and regional biomass burning aerosols is established. This results highlight that even distant biomass burning sources resulting from uncontrolled agricultural burns and deforestation negatively impact air quality in



densely populated areas hundreds of kilometers away, and that they do so in a regular basis. During our observation period, the maximum monthly-mean contribution of Brown Carbon to light-absorbing material was 13% .

335 *Data availability.* The data used in this article is available and will be provided upon request.

Author contributions. Conceptualization: R.M.B. and L.C.B., Investigation: J.M.R, M.A.R., M.Q.A. and A.P.S. Methodology: R.M.B., J.F.M. and A.P.S. Writing - Original Draft: J.M.R and R.M.B. Writing - review and editing: A.P.S., J.F.M. and L.C.B. Visualization: R.M.B., J.M.R. and M.A.R.

Competing interests. The authors declare that they have no conflict of interest.

340 *Acknowledgements.* This study was funded by the Colombian *Administrative Department of Science, Technology and Innovation - COL-CIENCIAS*, project No. 1204-745-56533 under grant contract No. FP44842-050-2017, and by the FAPA program from the Office of the vice-dean for Research from Universidad de los Andes. The authors thank the *Sanctuary of Monserrate* administration for kindly allowing the display of measurement devices and for providing sustained logistic support throughout the measurement period.



References

- 345 Akagi, S. K., Yokelson, R. J., Wiedinmyer, C., Alvarado, M. J., Reid, J. S., Karl, T., Crounse, J. D., and Wennberg, P. O.: Emission factors for open and domestic biomass burning for use in atmospheric models, *Atmos. Chem. Phys.*, 11, 4039–4072, <https://doi.org/10.5194/acp-11-4039-2011>, <https://www.atmos-chem-phys.net/11/4039/2011/>, 2011.
- Aurell, J. and Gullett, B. K.: Emission Factors from Aerial and Ground Measurements of Field and Laboratory Forest Burns in the Southeastern U.S.: PM_{2.5}, Black and Brown Carbon, VOC, and PCDD/PCDF, *Environ. Sci. Technol.*, 47, 8443–8452, <https://doi.org/10.1021/es402101k>, <http://pubs.acs.org/doi/abs/10.1021/es402101k>, 2013.
- 350 Birch, M. E. and Cary, R. A.: Elemental Carbon-Based Method for Monitoring Occupational Exposures to Particulate Diesel Exhaust, *Aerosol Sci. Tech.*, 25, 221–241, <https://doi.org/10.1080/02786829608965393>, 1996.
- Bond, T. C., Streets, D. G., Yarber, K. F., Nelson, S. M., Woo, J.-H., and Klimont, Z.: A technology-based global inventory of black and organic carbon emissions from combustion, *Journal of Geophysical Research: Atmospheres*, 109, <https://doi.org/10.1029/2003JD003697>, <https://agupubs.onlinelibrary.wiley.com/doi/abs/10.1029/2003JD003697>, 2004.
- 355 Bond, T. C., Doherty, S. J., Fahey, D. W., Forster, P. M., Berntsen, T., DeAngelo, B. J., Flanner, M. G., Ghan, S., Kärcher, B., Koch, D., Kinne, S., Kondo, Y., Quinn, P. K., Sarofim, M. C., Schultz, M. G., Schulz, M., Venkataraman, C., Zhang, H., Zhang, S., Bellouin, N., Guttikunda, S. K., Hopke, P. K., Jacobson, M. Z., Kaiser, J. W., Klimont, Z., Lohmann, U., Schwarz, J. P., Shindell, D., Storelvmo, T., Warren, S. G., and Zender, C. S.: Bounding the role of black carbon in the climate system: A scientific assessment, *J. Geophys. Res. Atmos.*, 118, 5380–5552, <https://doi.org/10.1002/jgrd.50171>, 2013.
- 360 Carslaw, D. C. and Ropkins, K.: openair - An R package for air quality data analysis, *Environ. Model. Softw.*, 27–28, 52–61, <https://doi.org/10.1016/j.envsoft.2011.09.008>, 2012.
- Chen, S., Russell, L., Cappa, C., Zhang, X., Kleeman, M., Kumar, A., Liu, D., and Ramanathan, V.: Comparing black and brown carbon absorption from AERONET and surface measurements at wintertime Fresno, *Atmos. Environ.*, 199, 164–176, <https://doi.org/10.1016/j.atmosenv.2018.11.032>, <https://linkinghub.elsevier.com/retrieve/pii/S1352231018308045>, 2018.
- 365 Cottle, P., Strawbridge, K., and McKendry, I.: Long-range transport of Siberian wildfire smoke to British Columbia: Lidar observations and air quality impacts, *Atmos. Environ.*, 90, 71–77, <https://doi.org/10.1016/j.atmosenv.2014.03.005>, 2014.
- Crutzen, P. J. and Andreae, M. O.: Biomass Burning in the Tropics : Impact on Atmospheric Chemistry and Biogeochemical Cycles, *Science*, 250, 1669–1678, <https://doi.org/10.1126/science.250.4988.1669>, 1991.
- 370 Cubison, M. J., Ortega, A. M., Hayes, P. L., Farmer, D. K., Day, D., Lechner, M. J., Brune, W. H., Apel, E., Diskin, G. S., Fisher, J. A., Fuelberg, H. E., Hecobian, A., Knapp, D. J., Mikoviny, T., Riemer, D., Sachse, G. W., Sessions, W., Weber, R. J., Weinheimer, A. J., Wisthaler, A., and Jimenez, J. L.: Effects of aging on organic aerosol from open biomass burning smoke in aircraft and laboratory studies, *Atmos. Chem. Phys.*, 11, 12 049–12 064, <https://doi.org/10.5194/acp-11-12049-2011>, <https://www.atmos-chem-phys.net/11/12049/2011/>, 2011.
- 375 de Oliveira Alves, N., Brito, J., Caumo, S., Arana, A., de Souza Hacon, S., Artaxo, P., Hillamo, R., Teinilä, K., de Medeiros, S. R. B., and de Castro Vasconcellos, P.: Biomass burning in the Amazon region: Aerosol source apportionment and associated health risk assessment, *Atmos. Environ.*, 120, 277 – 285, <https://doi.org/https://doi.org/10.1016/j.atmosenv.2015.08.059>, 2015.
- Donnelly, A. A., Broderick, B. M., and Misstear, B. D.: The effect of long-range air mass transport pathways on PM₁₀ and NO₂ concentrations at urban and rural background sites in Ireland: Quantification using clustering techniques, *J. Environ. Sci. Heal. Part A*, 50, 647–658, <https://doi.org/10.1080/10934529.2015.1011955>, <http://www.tandfonline.com/doi/full/10.1080/10934529.2015.1011955>, 2015.
- 380



- Draxler, R. and Hess, G.: An Overview of the HYSPLIT_4 Modelling System for Trajectories, Dispersion, and Deposition, *Aust. Meteorol. Mag.*, 47, 295–308, 1998.
- Drinovec, L., Močnik, G., Zotter, P., Prévôt, A. S. H., Ruckstuhl, C., Coz, E., Rupakheti, M., Sciare, J., Müller, T., Wiedensohler, A., and Hansen, A. D. A.: The "dual-spot" Aethalometer: An improved measurement of aerosol black carbon with real-time loading compensation, *Atmos. Meas. Tech.*, 8, 1965–1979, <https://doi.org/10.5194/amt-8-1965-2015>, <https://www.atmos-meas-tech.net/8/1965/2015/>, 2015.
- 385 Forster, C., Wandinger, U., Wotawa, G., James, P., Mattis, I., Althausen, D., Simmonds, P., O'Doherty, S., Jennings, S. G., Kleefeld, C., Schneider, J., Trickl, T., Kreipl, S., Jäger, H., and Stohl, A.: Transport of boreal forest fire emissions from Canada to Europe, *J. Geophys. Res.*, 106, 22 887–22 906, <https://doi.org/10.1029/2001JD900115>, 2001.
- Garcia-Hurtado, E., Pey, J., Borrás, E., Sánchez, P., Vera, T., Carratalá, A., Alastuey, A., Querol, X., and Vallejo, V. R.: Atmospheric PM and volatile organic compounds released from Mediterranean shrubland wildfires, *Atmos. Environ.*, 89, 85–92, <https://doi.org/10.1016/j.atmosenv.2014.02.016>, 2014.
- 390 Gonçalves, C., Figueiredo, B. R., Alves, C. A., Cardoso, A. A., Da Silva, R., Kanzawa, S. H., and Vicente, A. M.: Chemical characterisation of total suspended particulate matter from a remote area in Amazonia, *Atmos. Res.*, 182, 102–113, <https://doi.org/10.1016/J.ATMOSRES.2016.07.027>, <http://www.sciencedirect.com/ezproxy.uniandes.edu.co:8080/science/article/pii/S0169809516302071>, 2016.
- 395 Haikerwal, A., Akram, M., Del Monaco, A., Smith, K., Sim, M. R., Meyer, M., Tonkin, A. M., Abramson, M. J., and Dennekamp, M.: Impact of Fine Particulate Matter (PM_{2.5}) Exposure During Wildfires on Cardiovascular Health Outcomes., *J. Am. Heart Assoc.*, 4, e001 653, <https://doi.org/10.1161/JAHA.114.001653>, <http://www.ncbi.nlm.nih.gov/pubmed/26178402><http://www.pubmedcentral.nih.gov/articlerender.fcgi?artid=PMC4608063>, 2015.
- 400 Hamburger, T., Matisāns, M., Tunved, P., Ström, J., Calderon, S., Hoffmann, P., Hochschild, G., Gross, J., Schmeissner, T., Wiedensohler, A., and Krejci, R.: Long-term in situ observations of biomass burning aerosol at a high altitude station in Venezuela: Sources, impacts and interannual variability, *Atmos. Chem. Phys.*, 13, 9837–9853, <https://doi.org/10.5194/acp-13-9837-2013>, <http://www.atmos-chem-phys.net/13/9837/2013/>, 2013.
- Harrison, R. M., Beddows, D. C., Jones, A. M., Calvo, A., Alves, C., and Pio, C.: An evaluation of some issues regarding the use of Aethalometers to measure woodsmoke concentrations, *Atmos. Environ.*, 80, 540 – 548, <https://doi.org/https://doi.org/10.1016/j.atmosenv.2013.08.026>, 2013.
- 405 Hecobian, A., Zhang, X., Zheng, M., Frank, N., Edgerton, E. S., and Weber, R. J.: Water-Soluble Organic Aerosol material and the light-absorption characteristics of aqueous extracts measured over the Southeastern United States, *Atmos. Chem. Phys.*, 10, 5965–5977, <https://doi.org/10.5194/acp-10-5965-2010>, <https://www.atmos-chem-phys.net/10/5965/2010/>, 2010.
- 410 Hennigan, C. J., Sullivan, A. P., Collett Jr., J. L., and Robinson, A. L.: Levoglucosan stability in biomass burning particles exposed to hydroxyl radicals, *Geophys. Res. Lett.*, 37, <https://doi.org/10.1029/2010GL043088>, 2010.
- Hernandez, A. J., Morales-Rincon, L. A., W., D., Mallia, D., Lin, J., and Jimenez, R.: Transboundary transport of biomass burning aerosols and photochemical pollution in the Orinoco River Basin", *Atmos. Environ.*, 205, 1 – 8, <https://doi.org/https://doi.org/10.1016/j.atmosenv.2019.01.051>, <http://www.sciencedirect.com/science/article/pii/S1352231019300810>, 2019.
- 415 Janhäll, S., Andreae, M. O., and Pöschl, U.: Biomass burning aerosol emissions from vegetation fires: particle number and mass emission factors and size distributions, *Atmos. Chem. Phys.*, 10, 1427–1439, <https://doi.org/10.5194/acp-10-1427-2010>, <https://www.atmos-chem-phys.net/10/1427/2010/>, 2010.



- Jeong, C., Hopke, P., Kim, E., and Lee, D.: The comparison between thermal-optical transmittance Elemental Carbon and Aethalometer
420 Black Carbon measured at multiple monitoring sites, *Atmos. Environ.*, 38, 5193–5204, <https://doi.org/10.1016/j.atmosenv.2004.02.065>, 2004.
- Justice, C. O., Giglio, L., Korontzi, S., Owens, J., Morisette, J. T., Roy, D., Descloitres, J., Alleaume, S., Petitcolin, F., and Kaufman, Y.: The
MODIS fire products, *Remote Sens. Environ.*, 83, 244–262, [https://doi.org/10.1016/S0034-4257\(02\)00076-7](https://doi.org/10.1016/S0034-4257(02)00076-7), 2002.
- Kirchstetter, T. W., Novakov, T., and Hobbs, P. V.: Evidence that the spectral dependence of light absorption by aerosols is affected by organic
425 carbon, *Geophysical Research*, 109, 1–12, <https://doi.org/10.1029/2004JD004999>, 2004.
- Koch, D., Bond, T. C., Streets, D., Unger, N., and van der Werf, G. R.: Global impacts of aerosols from particular source regions and sectors,
J. Geophys. Res., 112, D02 205, <https://doi.org/10.1029/2005JD007024>, <http://doi.wiley.com/10.1029/2005JD007024>, 2007.
- Kollanus, V., Tiittanen, P., Niemi, J. V., and Lanki, T.: Effects of long-range transported air pollution from vegetation
fires on daily mortality and hospital admissions in the Helsinki metropolitan area, Finland, *Environ. Res.*, 151, 351–358,
430 <https://doi.org/10.1016/J.ENVRES.2016.08.003>, <http://www.sciencedirect.com/science/article/pii/S001393511630353X?via%3Dihub>, 2016.
- Lack, D. A. and Langridge, J. M.: On the attribution of black and brown carbon light absorption using the Ångström exponent, *Atmos. Chem. Phys.*, 13, 10 535–10 543, <https://doi.org/10.5194/acp-13-10535-2013>, <https://www.atmos-chem-phys.net/13/10535/2013/>, 2013.
- 435 Lack, D. A., Bahreini, R., Langridge, J. M., Gilman, J. B., and Middlebrook, A. M.: Brown carbon absorption linked to organic mass tracers in biomass burning particles, *Atmos. Chem. Phys.*, 13, 2415–2422, <https://doi.org/10.5194/acp-13-2415-2013>, <https://www.atmos-chem-phys.net/13/2415/2013/>, 2013.
- Laskin, A., Laskin, J., and Nizkorodov, S. A.: Chemistry of Atmospheric Brown Carbon, *Chemical Reviews*, 115, 4335–4382, <https://doi.org/10.1021/cr5006167>, 2015.
- 440 Marengo, J. A., Tomasella, J., Alves, L. M., Soares, W. R., and Rodriguez, D. A.: The drought of 2010 in the context of historical droughts in the Amazon region, *Geophysical Research Letters*, 38, <https://doi.org/10.1029/2011GL047436>, <https://agupubs.onlinelibrary.wiley.com/doi/abs/10.1029/2011GL047436>, 2011.
- Martinsson, J., Azeem, H. A., Sporre, M. K., Bergström, R., Ahlberg, E., and Öström, E.: Carbonaceous Aerosol Source Apportionment Using the Aethalometer Model – evaluation by radiocarbon and levoglucosan analysis at a rural background site in southern Sweden,
445 *Atmos. Chem. Phys.*, 17, 4265–4281, 2017.
- Massabò, D., Caponi, L., Bernardoni, V., Bove, M., Brotto, P., Calzolari, G., Cassola, F., Chiari, M., Fedi, M., Fermo, P., Giannoni, M., Lucarelli, F., Nava, S., Piazzalunga, A., Valli, G., Vecchi, R., and Prati, P.: Multi-wavelength optical determination of black and brown carbon in atmospheric aerosols, *Atmos. Environ.*, 108, 1 – 12, <https://doi.org/https://doi.org/10.1016/j.atmosenv.2015.02.058>, <http://www.sciencedirect.com/science/article/pii/S1352231015001831>, 2015.
- 450 Mendez-Espinosa, J., Belalcazar, L., and Morales Betancourt, R.: Regional Air Quality Impact of Northern South America Biomass Burning Emissions, *Atmos. Environ.*, 203, 131 – 140, <https://doi.org/https://doi.org/10.1016/j.atmosenv.2019.01.042>, <http://www.sciencedirect.com/science/article/pii/S135223101930072X>, 2019.
- Pachón, J. E., Weber, R. J., Zhang, X., Mulholland, J. A., and Russell, A. G.: Revising the use of potassium (K) in the source apportionment of PM_{2.5}, *Atmospheric Pollution Research*, 4, 14 – 21, <https://doi.org/https://doi.org/10.5094/APR.2013.002>, <http://www.sciencedirect.com/science/article/pii/S1309104215303962>, 2013.
- 455



- Pachón, J. E., Galvis, B., Lombana, O., Carmona, L. G., Fajardo, S., Rincón, A., Meneses, S., Chaparro, R., Nedbor-Gross, R., and Henderson, B.: Development and Evaluation of a Comprehensive Atmospheric Emission Inventory for Air Quality Modeling in the Megacity of Bogotá, *Atmosphere*, 9, <https://doi.org/10.3390/atmos9020049>, <http://www.mdpi.com/2073-4433/9/2/49>, 2018.
- Petzold, A., Ogren, J. A., Fiebig, M., Laj, P., Li, S.-M., Baltensperger, U., Holzer-Popp, T., Kinne, S., Pappalardo, G., Sugimoto, N., Wehrli, C., Wiedensohler, A., and Zhang, X.-Y.: Recommendations for reporting "black carbon" measurements, *Atmos. Chem. Phys.*, 13, 8365–8379, <https://doi.org/10.5194/acp-13-8365-2013>, <https://www.atmos-chem-phys.net/13/8365/2013/>, 2013.
- Phuleria, H. C., Fine, P. M., Zhu, Y. F., and Sioutas, C.: Air quality impacts of the October 2003 Southern California wildfires, *J. Geophys. Res.*, 110, D07S20–D07S20, <https://doi.org/10.1029/2004JD004626>, <http://onlinelibrary.wiley.com/doi/10.1029/2004JD004626/full>, 2005.
- Poveda, G., Waylen, P. R., and Pulwarty, R. S.: Annual and inter-annual variability of the present climate in northern South America and southern Mesoamerica, *Palaeogeography, Palaeoclimatology, Palaeoecology*, 234, 3 – 27, <https://doi.org/https://doi.org/10.1016/j.palaeo.2005.10.031>, late Quaternary climates of tropical America and adjacent seas, 2006.
- Prenni, A. J., Demott, P. J., Sullivan, A. P., Sullivan, R. C., Kreidenweis, S. M., and Rogers, D. C.: Biomass burning as a potential source for atmospheric ice nuclei: Western wildfires and prescribed burns, *Geophysical Research Letters*, 39, 1–5, <https://doi.org/10.1029/2012GL051915>, 2012.
- Pulwarty, R. S., Barry, R. G., Hurst, C. M., Sellinger, K., and Mogollon, L. E.: Meteorology , and Atmospheric Physics Precipitation in the Venezuelan Andes in the Context of Regional Climate, *Meteorology and Atmospheric Physics*, 237, 217–237, 1998.
- Reid, C. E., Jerrett, M., Tager, I. B., Petersen, M. L., Mann, J. K., and Balmes, J. R.: Differential respiratory health effects from the 2008 northern California wildfires: A spatiotemporal approach, *Environ. Res.*, 150, 227–235, <https://doi.org/10.1016/J.ENVRES.2016.06.012>, <http://www.sciencedirect.com.ezproxy.uniandes.edu.co:8080/science/article/pii/S001393511630247X?via%3Dihub>, 2016.
- Sandradewi, J., Prévot, A. S. H., Szidat, S., Perron, N., Alfarra, M. R., Lanz, V. A., Weingartner, E., and Baltensperger, U.: Using Aerosol Light Absorption Measurements for the Quantitative Determination of Wood Burning and Traffic Emission Contributions to Particulate Matter, *Environmental Science & Technology*, 42, 3316–3323, <https://doi.org/10.1021/es702253m>, <https://doi.org/10.1021/es702253m>, PMID: 18522112, 2008.
- Schmeissner, T., Krejci, R., Ström, J., Birmili, W., Wiedensohler, A., Hochschild, G., Gross, J., Hoffmann, P., and Calderon, S.: Analysis of number size distributions of tropical free tropospheric aerosol particles observed at Pico Espejo (4765 m a.s.l.), Venezuela, *Atmos. Chem. Phys.*, 11, 3319–3332, <https://doi.org/10.5194/acp-11-3319-2011>, <https://www.atmos-chem-phys.net/11/3319/2011/>, 2011.
- Shen, Z., Zhang, Q., Cao, J., Zhang, L., Lei, Y., Huang, Y., Huang, R., Gao, J., Zhao, Z., Zhu, C., Xiuli, Y., Zheng, C., Xu, H., and Liu, S.: Optical properties and possible sources of brown carbon in PM_{2.5} over Xian, China, *Atmos. Environ.*, 150, 322–330, <https://doi.org/10.1016/j.atmosenv.2016.11.024>, <http://dx.doi.org/10.1016/j.atmosenv.2016.11.024>, 2017.
- Simoneit, B., Schauer, J., Nolte, C., Oros, D., Elias, V., Fraser, M., Rogge, W., and Cass, G.: Levoglucosan, a tracer for cellulose in biomass burning and atmospheric particles, *Atmos. Environ.*, 33, 173 – 182, [https://doi.org/https://doi.org/10.1016/S1352-2310\(98\)00145-9](https://doi.org/https://doi.org/10.1016/S1352-2310(98)00145-9), 1999.
- Stein, A. F., Draxler, R. R., Rolph, G. D., Stunder, B. J., Cohen, M. D., and Ngan, F.: NOAA's HYSPLIT atmospheric transport and dispersion modeling system, *Bull. Am. Meteorol.*, 96, 2059–2077, <https://doi.org/10.1175/BAMS-D-14-00110.1>, 2015.
- Stohl, A., Aamaas, B., Amann, M., Baker, L. H., Bellouin, N., Berntsen, T. K., Boucher, O., Cherian, R., Collins, W., Daskalakis, N., Dusinska, M., Eckhardt, S., Fuglestedt, J. S., Harju, M., Heyes, C., Hodnebrog, Hao, J., Im, U., Kanakidou, M., Klimont, Z., Kupiainen, K., Law, K. S., Lund, M. T., Maas, R., MacIntosh, C. R., Myhre, G., Myriokefalitakis, S., Olivie, D., Quaas, J., Quennehen, B., Raut, J. C., Rumbold, S. T., Samset, B. H., Schulz, M., Seland, Shine, K. P., Skeie, R. B., Wang, S., Yttri, K. E., and Zhu, T.: Evaluating the climate



- and air quality impacts of short-lived pollutants, *Atmos. Chem. Phys.*, 15, 10 529–10 566, <https://doi.org/10.5194/acp-15-10529-2015>,
495 2015.
- Su, L., Yuan, Z., Fung, J. C., and Lau, A. K.: A comparison of HYSPLIT backward trajectories generated from two GDAS datasets, *Sci. Total Environ.*, 506–507, 527–537, <https://doi.org/10.1016/J.SCITOTENV.2014.11.072>, 2015.
- Sullivan, A. P. and Weber, R. J.: Chemical characterization of the ambient organic aerosol soluble in water: 1. Isolation of hydrophobic and hydrophilic fractions with a XAD-8 resin, *J. Geophys. Res.*, 111, <https://doi.org/10.1029/2005JD006485>, 2006a.
- 500 Sullivan, A. P. and Weber, R. J.: Chemical characterization of the ambient organic aerosol soluble in water: 2. Isolation of acid, neutral, and basic fractions by modified size-exclusion chromatography, *J. Geophys. Res.*, 111, <https://doi.org/10.1029/2005JD006486>, 2006b.
- Sullivan, A. P., Holden, A. S., Patterson, L. A., McMeeking, G. R., Kreidenweis, S. M., Malm, W. C., Hao, W. M., Wold, C. E., and Collett Jr., J. L.: A method for smoke marker measurements and its potential application for determining the contribution of biomass burning from wildfires and prescribed fires to ambient PM_{2.5} organic carbon, *Journal of Geophysical Research: Atmospheres*, 113,
505 <https://doi.org/10.1029/2008JD010216>, 2008.
- Sullivan, A. P., Frank, N., Kenski, D. M., and Collett, J. L.: Application of high-performance anion-exchange chromatography-pulsed amperometric detection for measuring carbohydrates in routine daily filter samples collected by a national network: 1 Determination of the impact of biomass burning in the upper Midwest, *J. Geophys. Res.*, 116, <https://doi.org/10.1029/2010JD014169>, 2011.
- Thornhill, G. D., Ryder, C. L., Highwood, E. J., Shaffrey, L. C., and Johnson, B. T.: The Effect of South American Biomass Burning
510 Aerosol Emissions on the Regional Climate, *Atmos. Chem. Phys. Discuss.*, pp. 1–34, <https://doi.org/10.5194/acp-2017-953>, <https://www.atmos-chem-phys-discuss.net/acp-2017-953/>, 2017.
- Tsimpidi, A. P., Karydis, V. A., Pandis, S. N., and Lelieveld, J.: Global combustion sources of organic aerosols: model comparison with 84 AMS factor-analysis data sets, *Atmos. Chem. Phys.*, 16, 8939–8962, <https://doi.org/10.5194/acp-16-8939-2016>, 2016.
- Tzompa-Sosa, Z. A., Sullivan, A. P., Retama, A., and Kreidenweis, S. M.: Contribution of Biomass Burning to Carbonaceous Aerosols in
515 Mexico City during May 2013, *Aerosol and Air Quality Research*, 16, 114–124, <https://doi.org/10.4209/aaqr.2015.01.0030>, 2016.
- van der Werf, G. R., Randerson, J. T., Giglio, L., Collatz, G. J., Mu, M., Kasibhatla, P. S., Morton, D. C., DeFries, R. S., Jin, Y., and van Leeuwen, T. T.: Global fire emissions and the contribution of deforestation, savanna, forest, agricultural, and peat fires (1997–2009), *Atmos. Chem. Phys.*, 10, 11 707–11 735, <https://doi.org/10.5194/acp-10-11707-2010>, <https://www.atmos-chem-phys.net/10/11707/2010/>, 2010.
- 520 Virkkula, A., Mäkelä, T., Hillamo, R., Yli-Tuomi, T., Hirsikko, A., Hämeri, K., and Koponen, I.: A Simple Procedure for Correcting Loading Effects of Aethalometer Data, *J. Air & Waste Manage. Assoc.*, 57, 1214–1222, <https://doi.org/10.3155/1047-3289.57.10.1214>, 2007.
- Wang, J., Nie, W., Cheng, Y., Shen, Y., Chi, X., Wang, J., Huang, X., Xie, Y., Sun, P., Xu, Z., Qi, X., Su, H., and Ding, A.: Light absorption of brown carbon in eastern China based on 3-year multi-wavelength aerosol optical property observations and an improved absorption Ångström exponent segregation method, *Atmos. Chem. Phys.*, 18, 9061–9074, <https://doi.org/10.5194/acp-18-9061-2018>, 2018.
- 525 Weber, R. J., Sullivan, A. P., Peltier, R. E., Russell, A., Yan, B., Zheng, M., de Gouw, J., Warneke, C., Brock, C., Holloway, J. S., Atlas, E. L., and Edgerton, E.: A study of secondary organic aerosol formation in the anthropogenic-influenced southeastern United States, *J. Geophys. Res.*, 112, <https://doi.org/10.1029/2007JD008408>, 2007.
- Wong, J. P., Tsagkaraki, M., Tsiotra, I., Mihalopoulos, N., Violaki, K., Kanakidou, M., Sciare, J., Nenes, A., and Weber, R. J.: Effects of Atmospheric Processing on the Oxidative Potential of Biomass Burning Organic Aerosols, *Environmental Science & Technology*, 53,
530 6747–6756, <https://doi.org/10.1021/acs.est.9b01034>, <https://doi.org/10.1021/acs.est.9b01034>, PMID: 31091086, 2019.



- Yamasoe, M. A., Artaxo, P., Miguel, A. H., and Allen, A. G.: Chemical composition of aerosol particles from direct emissions of vegetation fires in the Amazon Basin: water-soluble species and trace elements, *Atmos. Environ.*, 34, 1641 – 1653, [https://doi.org/https://doi.org/10.1016/S1352-2310\(99\)00329-5](https://doi.org/https://doi.org/10.1016/S1352-2310(99)00329-5), 2000.
- 535 Youssef, H., Lioussé, C., Roblou, L., Assamoi, E. M., Salonen, R. O., Maesano, C., Banerjee, S., and Annesi-Maesano, I.: Quantifying wildfires exposure for investigating health-related effects, <https://doi.org/10.1016/j.atmosenv.2014.07.041>, 2014.